

# NUMERICAL AND EXPERIMENTAL INVESTIGATION OF A MICRO GAS TURBINE COMBUSTION CHAMBER

Andreea Cristina Mangra, Razvan Carlanescu, Marius Enache, Florin Florean, Radu Kuncser

National Research & Development Institute for Gas Turbines COMOTI,  
220 D Iuliu Maniu Bd., sector 6, 061126 Bucharest, Romania

Corresponding author: Andreea Cristina Mangra, [andreea.petcu@comoti.ro](mailto:andreea.petcu@comoti.ro)

**Abstract:** Micro gas - turbines (MGT) offer many advantages such as higher thermal efficiency and reduced noise, and are suitable sources for power generation due to their fuel flexibility, small sizes, and high efficiencies. In recent years, there has been an increase interest in developing MGT for transportation platforms such as Range Extender for Electric Vehicle (REEV), Unmanned Ground/Air Vehicles (UGV/UAV), Auxiliary Power Units (APU). For these applications, the MGT must meet essential requirements like reliability, reasonable price, ecological safety, low noise and vibration, multi-fuel, etc. This paper presents the numerical and experimental investigation of a newly designed annular type combustion chamber. This combustion chamber is part of a 40 daN micro gas turbine, destined to equip a small-scale multifunctional airplane. The combustion chamber is equipped with six innovative vaporizers, using Jet-A as fuel, patented by INCDT COMOTI. The experimental installation on which the combustion tests have been performed consists of: the fuel supply system, an air source, the combustion chamber assembly, a chimney for flue gas exhaust. During the combustion chamber testing campaign, the following parameters have been monitored and registered: air mass flow, air temperature, and pressure before the combustion chamber entrance, the temperature at the combustion chamber exit, the temperature before the pressure regulating valve placed on the exhaust pipe. After the testing campaign has been concluded the numerical simulations have been resumed. A three-dimensional RANS numerical integration of the Navier-Stokes equations has been carried out, using an Eddy Dissipation Combustion Model (EDM) and the  $k-\epsilon$  turbulence model, implemented in a numerical simulation conducted using the commercial software ANSYS CFX. The computational domain has been modified in order to match the testing rig. Due to the complex geometry of the computational domain, an unstructured type computational grid has been used. The imposed boundary conditions have been changed in order to match the testing conditions and functioning regimes. A kerosene – air two steps reaction mechanism, with NO formation, has been used. The numerical simulation results have been compared with the parameters measured experimentally, thus validating the obtained results.

**Key words:** micro gas turbine, numerical simulation, combustion chamber, ANSYS CFX.

## 1. INTRODUCTION

This paper presents the numerical and experimental investigation of a newly designed annular-type combustion chamber. This combustion chamber is part of a 40 daN micro gas turbine, destined to equip a small-scale multifunctional airplane. The combustion chamber is equipped with six innovative vaporizers, using Jet-A as fuel, patented by INCDT COMOTI [1]. The need to achieve certain combustor requirements has led to the technical solution of using vaporizers in gas turbine combustors instead of atomizers. Vaporizers are documented to have been used in gas turbine combustors as early as 1941 [2]. Whittle [2] had reported that vaporizers provided adequate performance, but were prone to thermal cracking and blockage. Trying to solve these issues has led to the development of vaporizer solutions, resulting in simplifying and enhancing vaporizer technology. Vaporizers have a double purpose, firstly to vaporize the liquid fuel and secondly, to disperse the reactive air-fuel mixture within the combustion chamber. Vaporization is achieved by transferring heat from the hot combustion gases to the fuel. Positioning the outlet of the vaporizer within the primary combustion zone facilitates the dispersion the reactive air-fuel mixture within the combustion chamber. In the scientific literature different vaporizers geometries can be found. In [3] three vaporizer geometries have been experimentally studied. The results show that the guide vane configuration has had a wider spray angle than the straight tube configuration.

Vaporizers have significant advantages over pressure swirl atomizers and air blast atomizers when considering micro gas turbine applications. The most significant of these advantages is the reduction of the combustion chamber's dimensions. This is due to the injection of combustion reactants within the primary combustion zone which results in improved mixing and reaction speed [4]. This is confirmed numerically and experimentally [5,6,7]. Fuel injection pressures

are also greatly reduced compared to pressure atomizers and air blast atomizers. Thus, fuel pumps can achieve a wider operational flow range and the rest of the fuel system operates with reduced stress loading. The reduced stress on components results in reduced maintenance, less expensive designs due to lower strength requirements and lead to reduced overall component weight. The main disadvantages of vaporizers occur during start-up and re-ignition [4]. An ignitable mixture cannot be produced by the vaporizers by themselves. Thus, for start-up, a pilot flame, generated by a glow plug, can be used, or the combustor can be equipped with a gaseous fuel supply ramp.

The designed annular-type combustion chamber is part of a micro gas turbine equipped with a one-stage centrifugal compressor and a one-stage axial turbine. For start-up, the combustion chamber is equipped with a gaseous fuel ramp. The ignition is done using a spark plug. After the vaporizers and the fire tube walls are heated, the liquid fuel is sprayed from the main fuel supply ramp into the vaporizers which are positioned inside the fire tube. The vaporizers' pre-heated walls facilitate the fuel droplets vaporization before passing into the fire tube. The pressurized air coming from the compressor enters the fire tube, forming with the fuel vapours a reactive mixture. By combustion, the fuel's chemical energy is transformed into heat. Mechanical work is produced by the resulted exhaust gases expansion through the turbine.

Micro gas turbines (MGT) have been used in multiple applications due to their fuel flexibility, small sizes, and high efficiencies [8]. Studying the trends in MGTs operating around the world reveals that the demand is growing rapidly [9]. MGTs will be used more and more for powering missiles, Unmanned Aerial Vehicles (UAVs), experimental vehicles like jetpacks, etc. The UAVs and drone market has seen several MGT units in development. This is due to the demand for quieter, lighter, and more efficient engines to replace the commonly used piston engine [10]. Examples of such projects include the US Navy Black Ghost [11] (<20 kW) engine for small drones, the TJ40-G1 [12] turbojet engine developed by PBS Aerospace for small aircrafts such as gliders or some larger model aircraft, and the Monarch 5 [13], which has been developed by UAV Turbines for powering a turboprop system or working as a range extender for small electrical hybrid aerial vehicles.

## 2. EXPERIMENTAL TESTING RIG

The experimenting campaign has taken place in INCDT COMOTI Combustion Chamber Laboratory. The testing rig on which the experimenting campaign has been conducted, consists of: an air source, a tank of gaseous fuel (used for starting the micro gas

turbine), liquid fuel supply system, compressor stator and combustion chamber assembly, butterfly valve for pressure regulation, an air compressor for butterfly valve actuation, exhaust gases chimney. A diagram of the testing line is presented in figure 1. In figure 2 are presented the compressor stator/combustion chamber assembly and the butterfly valve installed on the testing line. The existent control system and the data acquisition and monitoring software have been adapted for this application.

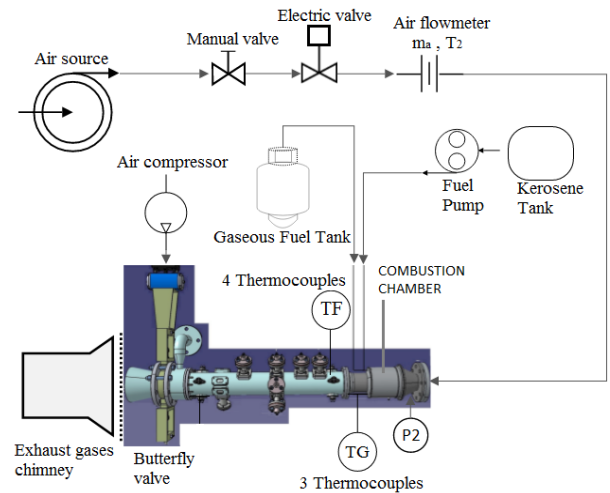


Fig 1. Testing line diagram



Fig. 2. Combustion chamber assembly and pressure regulation valve

Table 1 presents the parameters monitored and recorded during the tests and the used instrumentation. Combustion tests have been conducted both at atmospheric pressure (the butterfly valve completely opened) and at high pressure (the butterfly position has been varied). Different functioning regimes have been tested by varying the air mass flow and fuel mass flow, keeping the flue gases temperature at the combustion chamber exit under 900°C. The air mass flow has been set using the electric valve installed on the air supply line. The combustion chamber was first supplied with propane from a gas tank. The air/fuel mixture was ignited with a spark plug.

Table 1. Testing rig instrumentation

Parameter	Unit	Instrumentation	Position
Fuel pump speed	rpm	Variable speed Titan fuel pump	Fuel supply line
Air mass flow	kg/s	Orifice plate (DN80, PN16), accuracy $\pm 0.0375\%$	Air supply line
Air temperature ( $T_2$ )	$^{\circ}\text{C}$	Temperature transducer TR Pt 100, $T_{\text{max}}=250^{\circ}\text{C}$ , accuracy $\pm 1\%$	Air supply line
Air pressure ( $P_2$ )	bar	ST3000 Smart Pressure Transmitter (Honeywell), accuracy $\pm 0.0375\%$	Compressor stator inlet
Flue gases temperature ( $T_{G1}$ , $T_{G2}$ , $T_{G3}$ )	$^{\circ}\text{C}$	Thermocouple type K, $T_{\text{max}}=1200^{\circ}\text{C}$ , accuracy $\pm 1\%$	Combustion chamber outlet
Flue gases temperature ( $T_{F1}$ , $T_{F2}$ , $T_{F3}$ , $T_{F4}$ )	$^{\circ}\text{C}$	Thermocouple type K, $T_{\text{max}}=1200^{\circ}\text{C}$ , accuracy $\pm 1\%$	Upstream the butterfly valve
Butterfly valve position	% open	Electro-pneumatic positioner, $P_{\text{max}}=10\text{bar}$ , $T_{\text{max}}=80^{\circ}\text{C}$	Exhaust gases outlet

After the flame has stabilized and the vaporizers and fire tube walls have reached a high enough temperature that facilitates vaporization, the fire tube has been supplied with liquid fuel (Jet A). A variable speed gear liquid fuel pump, powered by a 6VDC power source, has been used. The fuel mass flow has been modified by varying the power source output voltage. The gaseous fuel has been used only for start-up.

### 3. NUMERICAL SIMULATION SETTINGS

After the testing campaign has been concluded the numerical simulations have been resumed. The commercial software ANSYS CFX has been used to perform a 3D steady RANS numerical simulation of the complex phenomena taking place inside the tested combustion chamber.

#### 3.1 Geometry and mesh

The geometry of the computational domain has been created using 3D design software CATIA, based on the configuration of the testing rig. In the design stage of the fire tube, the computational domain included only the combustion chamber assembly, starting from the compressor's stator exit and ending at the turbine stator entrance. Now, the computational domain has been modified in order to match the testing rig. In addition to the combustion chamber assembly (figure 3), the computational domain includes the compressor stator, the cone connecting the air supply line to the compressor stator, and the pipe section with the pressure regulation valve.

Due to the complex geometry of the computational domain, an unstructured type computational grid has been generated using ICEM CFD. The mesh has 11.597.711 elements and 1.989.593 nodes (figure 4). The mesh has been refined inside the fire tube, in the primary zone, as it can be seen in figure 5.

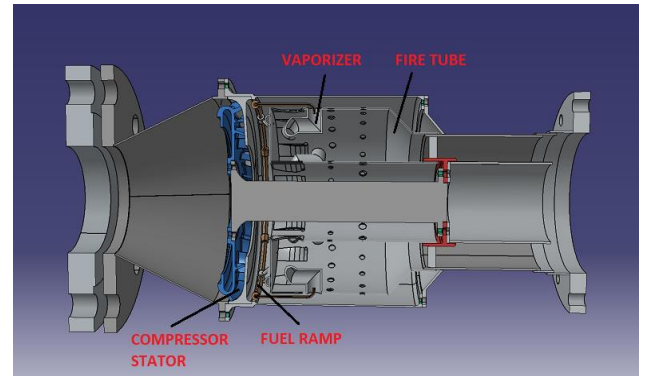


Fig. 3. The Combustion chamber assembly and compressor stator

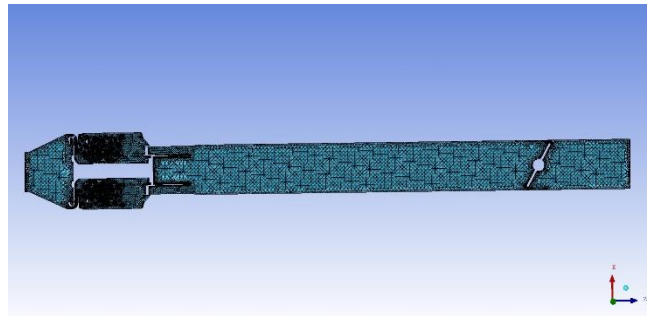


Fig. 4. The mesh on a section plane along the computational domain

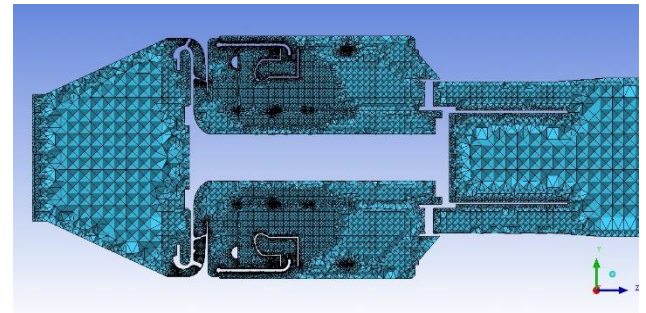


Fig. 5. Detail of the mesh inside the combustion chamber assembly

### 3.2 Boundary conditions

In order to validate the numerical simulation results, one of the functioning regimes from the experimental campaign has been considered. The imposed boundary conditions have been set in order to match the considered functioning regime (figure 6).

The atmospheric pressure of 101.325 Pa has been set as reference pressure. The air inlet has been considered the entrance in the cone connecting the compressor stator to the air supply line. The air mass flow and temperature have been imposed. The fuel is introduced in the computational domain through 6 surfaces of  $\phi$  0.6 mm, representing the outlet of the fuel supply ramp, one for each vaporizer. The Particle Transport Fluid morphology option has been selected for the fuel. An initial fuel droplet diameter of 100  $\mu$ m has been imposed. The fuel mass flow and temperature have been set. The fuel droplets atomization process has been modelled using the CAB (Cascade Atomization Break-up) model, available in ANSYS library. The fuel droplets vaporization process has been modelled using the Liquid Evaporation Model available in ANSYS library. The walls have been considered adiabatic. At the outlet, the atmospheric pressure has been imposed.

Being a RANS type simulation, the k- $\epsilon$  turbulence model have been chosen. This model has proven to be numerically stable and robust. Many researchers have used it in the realization of various technical applications numerical simulations, [14-16].

The chosen combustion model has been the Eddy Dissipation Model (EDM), based on a kerosene – air

two steps reaction mechanism, with NO formation, imported from the ANSYS library. As the pollutant emissions level was not of interest at this moment, a simple reaction mechanism has been chosen. Researchers prefer using this model due to its simplicity and robust performance in predicting turbulent reacting flows [16-18].

Three temperature monitoring points have been placed at the combustion chamber exit (figure 6), corresponding to the three thermocouples TG<sub>1</sub>, TG<sub>2</sub>, and TG<sub>3</sub> on the testing rig. Also, four temperature monitoring points have been placed before the pressure regulation valve (figure 6), corresponding to the four thermocouples TF<sub>1</sub>, TF<sub>2</sub>, TF<sub>3</sub>, and TF<sub>4</sub> on the testing rig.

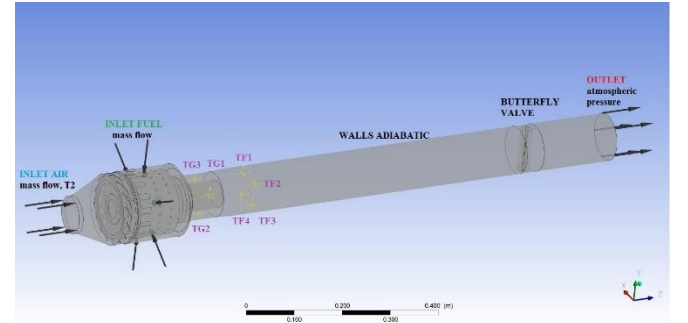


Fig. 6. Boundary conditions

## 4. RESULTS AND DISCUSSIONS

Table 2 presents the parameters monitored and registered for the considered functioning regime, chosen for validating the numerical results:

Table 2. Experimental data

Parameter	Valve position % open	T <sub>2</sub>	P <sub>2</sub>	Air mass flow	TG <sub>1</sub>	TG <sub>2</sub>	TG <sub>3</sub>	TG <sub>m</sub>	TF <sub>1</sub>	TF <sub>2</sub>	TF <sub>3</sub>	TF <sub>4</sub>	TF <sub>m</sub>
Unit		°C	bar	kg/s	°C	°C	°C	°C	°C	°C	°C	°C	°C
1	33	23.6	4.39	0.5804	804.5	757.4	545.3	702.4	616	709.1	883.4	760.9	742.4
2	33	23.6	4.39	0.5808	798	754.6	543.9	698.9	613.9	703.5	876.4	757.8	737.9
3	32.5	23.5	4.39	0.5809	799.8	753.6	545.3	699.6	610.8	700.4	874.3	755	735.1
4	32.6	23.6	4.39	0.5813	798.4	754.3	543.6	698.8	607.6	697.6	871.9	752.9	732.5
5	33	23.5	4.39	0.5813	798.4	754.3	543.9	698.9	602.4	695.8	870.8	752.2	730.3
6	32.9	23.6	4.39	0.5814	797.3	755.3	542.9	698.5	601.3	694.8	870.5	751.5	729.5
7	33.1	23.5	4.39	0.5823	795.9	755.3	543.3	698.2	599.6	693.4	869.1	750.1	728
8	32.7	23.6	4.39	0.5825	796.6	757.1	544.6	699.5	600.3	693	868	749.8	727.8
9	33.1	23.6	4.39	0.582	795.6	757.4	547.1	700	602.4	691.3	867.7	749	727.6
10	32.8	23.6	4.39	0.5837	794.2	756	546.8	699	601	690.6	867.3	747.6	726.6
11	33.1	23.5	4.39	0.5836	792.4	755	544.6	697.4	608	690.6	865.6	747.3	727.9
12	32.5	23.6	4.39	0.5835	794.5	755	545	698.2	606.9	690.6	864.9	746.9	727.3
13	33.1	23.5	4.39	0.5828	794.2	756.4	545.7	698.8	611.8	689.5	863.8	746.6	728
14	32.8	23.6	4.39	0.5825	796.6	756.4	545.7	699.6	611.5	689.5	864.2	746.3	727.9
Average	32.87	23.56	4.39	0.582	796.8	755.5	544.8	699.1	606.6	694.9	869.8	750.9	730.6

The air excess has been determined using equation (1) [19]:

$$\alpha = \frac{H_i - c_{pg} \cdot T_3}{c_{pg} \cdot T_3 \cdot \min L - c_{pa} \cdot T_2 \cdot \min L} \quad (1)$$

where  $H_i$  is the inferior calorific power of the fuel,  $c_{pg}$  is the exhaust gases specific heat at constant pressure,  $c_{pa}$  is the air specific heat at constant pressure,  $T_2$  is the total temperature at compressor exit,  $T_3$  is the total temperature at the combustion chamber exit, and  $\min L$  is the theoretical air quantity necessary for complete

combustion of the fuel. In this case, the used fuel is Jet A. Thus,  $H_i$  is 42800kJ/kg and  $minL$  is 14.6. According to the data presented in Table x,  $T_2 = 296.56$  K and  $T_3 = TG_m = 972.12$  K. Replacing in equation (1), an excess of air of 3.35 is obtained. Using equation (2) [19]:

$$m_c = \frac{m_a}{\alpha \cdot minL} \quad (2)$$

where  $m_c$  is the fuel mass flow,  $m_a$  is the air mass flow,  $\alpha$  is the air excess, and  $minL$  is the theoretical air quantity necessary for complete combustion of the fuel, a fuel mass flow of 0.0119 kg/s has resulted.

According to the data presented in Table 2, for the considered functioning regime, the pressure regulation valve was opened 32.87%. This is equivalent to an angle of approximately  $29.5^\circ$ . Thus, in the computational domain, the valve has been positioned according to this angle value.

In figure 7 is presented the total pressure field on a longitudinal plane through the whole computational domain. In figure 8 is presented a detail of the total pressure field inside the fire tube. The total pressure values presented in figures 7 - 8 are relative to the reference pressure set at 101325 Pa.

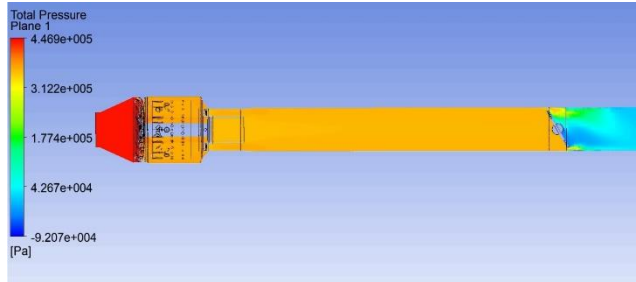


Fig. 7. Total pressure field on a longitudinal plane

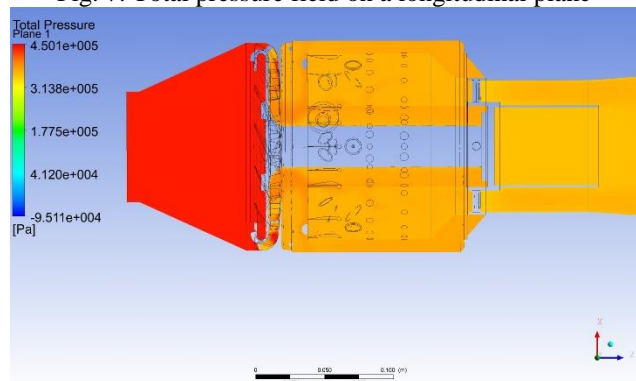


Fig. 8. Total pressure inside the fire tube

From figure 8 it can be observed a normal behaviour of the total pressure inside the fire tube. The total pressure decreases towards the fire tube exit.

From figures 9 - 12 it can be observed that the flame developed inside the fire tube, not exceeding its length. The flame developed in the central area of the fire tube, its walls not being subjected to high temperatures. The

temperature rises in the primary zone of the fire tube, as the combustion reaction takes place, reaching a maximum. The temperature then decreases in the secondary zone and the dilution zone of the fire tube. This is achieved by introducing a larger quantity of air through holes placed on the fire tube walls.

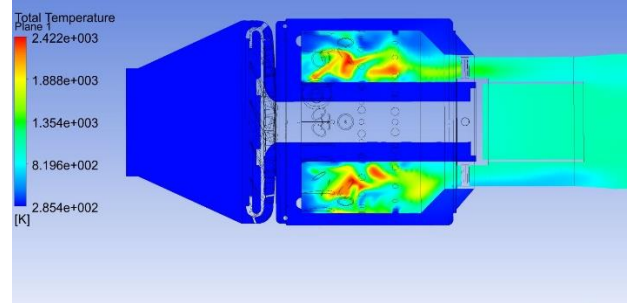


Fig. 9. Total temperature inside the fire tube

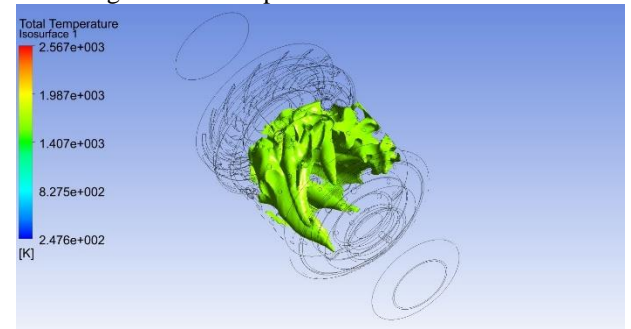


Fig. 10. 1600K total temperature isosurface

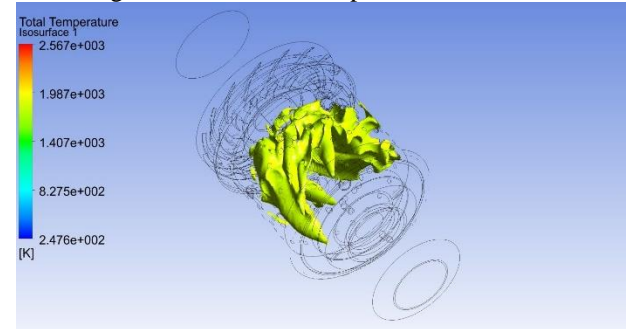


Fig. 11. 1800K total temperature isosurface

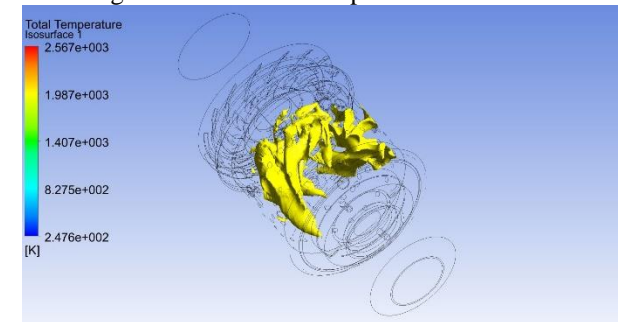


Fig. 12. 2000K total temperature isosurface

A comparison between the functioning parameters values obtained experimentally and through numerical simulation is presented in Table 3.  $TG_m$  and  $TF_m$  are compared with the average temperatures on the planes corresponding to  $TG_1$ ,  $TG_2$ , and  $TG_3$  monitoring points, respectively to  $TF_1$ ,  $TF_2$ ,  $TF_3$ , and  $TF_4$  monitoring points.

Table 3. Results comparison

Parameter	Experiment	Numerical simulation	Error
Air mass flow	0.582 kg/s	0.582 kg/s (imposed)	-
Air temperature ( $T_2$ )	23.5 °C	23.5 °C (imposed)	-
Fuel mass flow	0.0119 kg/s (calculated)	0.0119 kg/s (imposed)	-
Air pressure ( $P_2$ )	4.39 bar	4.38 bar	0.2 %
TGm ( $T_3$ )	699 °C	760 °C	8.7 %
TFm	730 °C	787 °C	7.8 %

As it can be seen from the data presented in Table 3, the numerical simulation results are validated by the experimental ones. The error between the results is under 10 % which is considered reasonable. The difference between the temperature values may be due to the imposed fuel mass flow. The fuel mass flow has been calculated, using equations 1 and 2, not measured. Thus, in the future the testing rig will be equipped with a fuel flow-meter. The numerical simulations will be resumed using as fuel mass flow the measured value.

## 5. CONCLUSIONS

A newly designed annular type combustion chamber, part of a 40 daN micro gas turbine, destined to equip a small-scale multifunctional airplane, has been numerically and experimentally investigated in INCDT COMOTI Combustion Chamber Laboratory.

The existent facility has been adapted in order to be able to test the designed combustion chamber. The functioning parameters monitored and registered during the experiments have been: the air mass flow, pressure ( $P_2$ ) and temperature ( $T_2$ ), the flue gases temperature ( $TG_1$ ,  $TG_2$ ,  $TG_3$ ) and pressure ( $P_3$ ) at the combustion chamber outlet, the pressure regulation valve position, and the flue gases temperature before the regulation valve ( $TF_1$ ,  $TF_2$ ,  $TF_3$ ,  $TF_4$ ).

In the design stage of the fire tube, the computational domain included only the combustion chamber assembly. After the testing campaign has been concluded, the computational domain has been modified in order to match the testing rig. This was done in order to be able to compare the numerical results with the experimental ones, thus validating them. The numerical simulations have been resumed, and the boundary conditions have been imposed in accordance with a chosen functioning regime. From the data presented in Table 3, it can be seen that between the experimental and numerical results there is a difference under 10%.

This shows that CFD techniques are reliable and have been proven very useful in designing different parts of a gas turbine, including the combustion chamber.

## 6. ACKNOWLEDGMENTS

This work has been carried out through Nucleu Program, with MCID support, project number PN 19.05.01.08.

## 7. REFERENCES

1. Carlanescu, R., Silivestru, V., Prisecaru, T., Carlanescu, C., Mangra, A., Florean, F., Kuncser, R., Enache, M., (2021). *Camera de ardere inelara policarburata cu vaporizare*, RO Patent OSIM A/00524.
2. Whittle, F., (1946). *The early history of the Whittle jet propulsion gas turbine*, Proc. of the Institution of Mechanical Engineering, 152, 419-435.
3. Jo, S., Joo, M., Choi, S., Dongho, R., (2019). Journal of ILASS-Korea, 24(3), 130-136.
4. Olivier, A.J., (2015). *An experimental and numerical investigation of vaporizer tubes associated with micro gas turbines*, Master Thesis, Stellenbosch University, South Africa.
5. Suchocki, T., Lampart, P., Klonowicz, P., (2015). J. Open Engineering, 5, 478-484.
6. Fuchs, F., Meidinger, V., Neuburger, N., Reiter, T., Zundel, M., Hupfer, A., (2016). *Challenges in designing very small jet engines – fuel distribution and atomization*, Int. Symp. on Transport Phenomena and Dynamics of Rotating Machinery, Hawaii, Honolulu, April 10-15 2016.
7. Mangra, A., (2020). Engineering, Technology & Applied Science Research, 10(6), 6422-6426.
8. Choi, M., Sung, Y., Won, M., Park, Y., Kim, M., Choi, G., Kim, D., (2017). *Effect of fuel distribution on turbulence and combustion characteristics of a micro gas turbine combustor*, J. Ind. Eng. Che., 48, 24-35.
9. Nozari, M., Tabejamaat, S., Sadeghizade, H., Aghayari, M., (2021). Energy, 235, 121372.
10. Adamou, A., Turner, J., Costall, A., Jones, A., Copeland, C., (2021). Energy Conversion and Management, 248, 114805.
11. Tuttle, S., Hinnant, K., Vick, M., (2017). *Preliminary Design, Ignition, and Fuel Injection for a High Temperature Recuperated Microturbine Combustor*, Proc. of the Asme Turbo Expo: Turbine Technical Conference and Exposition, Charlotte, USA, 26-30.06.2017, vol 4A: Combustion, Fuels and

## Emissions

12. PBS Aerospace, Available from: <https://www.pbsaerospace.com/aerospace-products/engines/turbojet-engines/tj-40-turbojet-engine-2>, 2022, Accessed 20.02.2022.
13. UAVTurbinesInc., UAV Turbines, Available from: <https://www.uavturbines.com/>, 2022, Accessed 20.02.2022.
14. Xing, C., Chen, X., Qiu, P., Liu, L., Yu, X., Zhao, Y., Zhang, L., Liu, J., Hu, Q., (2022). J of the Energy Institute, 102, 100-117.
15. Kurreck, M., Willmann, M., Wittig, S., (1998). J Eng Gas Turb Power, 120, 77-83.
16. Yilmaz, H., Cam, O., Tangoz, S., Yilmaz, I., (2017). Int J of Hydrogen Energy, 42(40), 25744-25755.
17. Li, L., Peng, X.F., Liu, T., (2006). Applied Thermal Engineering, 26(16), 1771-1779.
18. Agarwal, A., Pitso, I (2020). Materials Today: Proceedings, 27(2), 1341-1349.
19. Popa, B., Vintila, C., (1973). *Thermotechnics, machines and installations (Termotehnica, masini si instalatii – rom.)*,: Didactica si Pedagogica Publishing House, Bucharest.